Pramāna, Vol. 20, No. 4, April 1983, pp. 267–277. © Printed in India.

# Huang diffuse scattering from interstitials in a general orthorhombic and tetragonal lattice

RITA KHANNA
Materials Science Laboratory, Reactor Research Centre, Kalpakkam 603 102, India

MS received 25 August 1982

**Abstract.** Using the continuum theory of linear elasticity, Huang diffuse scattering (HDS) has been calculated from self-interstitials in a general orthorhombic and tetragonal lattice. Various defect configurations are represented according to the point group symmetry of the defect site. The contribution to HDS from all possible equivalent orientations (assumed to be equally populated) of the defect configuration is averaged. The limitations of HDS in discriminating between defect configurations having the same long-range symmetry are discussed, considering some special cases.

**Keywords.** Huang diffuse scattering; interstitials; orthorhombic lattice; tetragonal lattice; defect symmetry; isointensity surfaces.

## 1. Introduction

With the possibility of observing single point defects, diffuse x-ray scattering has become increasingly important in the structure determination of point defects in metals. While the diffuse scattering from point defects in cubic metals has been investigated extensively (Dederichs 1973; Haubold 1975), only recently attention has been paid to point defects in other Bravais lattices (Ehrhart and Schonfeld 1979). In this paper we present a calculation of Huang diffuse scattering (HDS) from self-interstitials in a general orthorhombic and tetragonal lattice. HDS, which appears close to the Bragg peaks, depends on the long-range displacement field of the concerned defect and can be calculated from the continuum theory of linear elasticity. Representing the stress field of an interstitital by a symmetric force dipole tensor, we write an expression for the Fourier transform of the elastic displacement field and use this to calculate the HDS.

For a low concentration $C$(number per unit volume) of point defects distributed at random, we assume a linear superposition of the strain fields around the point defects (the 'single defect approximation'). The diffuse x-ray scattering cross-section can be written as

$$I_D = C \mid F(\mathbf{Q}) \mid^2, \tag{1}$$

with

$$F(\mathbf{Q}) = f_Q^D + f \sum_n [\exp(i\mathbf{Q}\cdot\mathbf{u}_n) - 1 - i\mathbf{Q}\cdot\mathbf{u}_n] \exp(i\mathbf{Q}\cdot\bar{\mathbf{x}}_n)$$

$$+ if\,\mathbf{Q}\cdot\sum_n \mathbf{u}_n \exp(i\mathbf{Q}\cdot\bar{\mathbf{x}}_n) \tag{2}$$

$F(\mathbf{Q})$ is the defect structure factor, $f_Q^D$ represents the scattering at the defect and $f$ is the atomic form factor of the atoms in a perfect lattice. $\bar{\mathbf{x}}_n$ is the position vector of an atom $n$ in the average lattice, *i.e.* in a lattice homogeneously relaxed by all the defects in the crystal. $\mathbf{u}_n$ is the static displacement of an atom $n$ due to the defect singled out. The scattering vector $\mathbf{Q}$ satisfies the relation, $\mathbf{Q}=\mathbf{h}+\mathbf{q}$, where $\mathbf{h}$ is a reciprocal lattice vector and $\mathbf{q}$ a vector within the first Brillouin zone.

Close to Bragg peaks ($\mathbf{q} \ll \mathbf{h}$, $\mathbf{h} \approx \mathbf{Q}$), the leading term (third) of (1) varies as $1/q^2$ (HDS)

$$I_H = C \left| if\,\mathbf{h} \cdot \sum_n \mathbf{u}_n \exp\left(i\mathbf{Q}\cdot\bar{\mathbf{x}}_n\right)\right|^2. \tag{3}$$

The next order contribution to $I_D$, varying as $1/q$, comes from the interference of Huang scattering amplitude with the first two terms in (1). It makes diffuse scattering asymmetric about the Bragg peak and contains information about the Debye-Waller factor and the sign of the force dipole tensor of the defect. Contributions from this term can be neglected for very small values of q. In this paper, we restrict our attention to HDS.

## 2. Basic formulae

For a lattice containing more than one atom in the unit cell, the summation $n$ in (3) can be split into two sums: one over all the atoms in the unit cell ($k$) and the other over all the unit cells ($l$) of the lattice. $I_H$ then becomes

$$I_H = C \left| if\,\mathbf{h} \cdot \sum_l \sum_k \left(\mathbf{u}\,(lk) \exp\left\{i\mathbf{Q} \cdot [\mathbf{x}\,(l) + \mathbf{x}\,(k)]\right\}\right)\right|^2 \tag{4}$$

Since all the atoms in a unit cell will be displaced equally in the elastic displacement field of the point defect, $\mathbf{u}(lk)$ is independent of the sublattice index $k$ and may be replaced by $\mathbf{u}(l)$. (4) then reduces to

$$I_H = C \left| i\left(f \sum_k \exp\left[i\mathbf{h} \cdot \mathbf{x}\,(k)\right]\right) \mathbf{h} \cdot \sum_l \mathbf{u}\,(l) \exp\left[i\mathbf{q} \cdot \mathbf{x}\,(l)\right]\right|^2$$

$$\approx C \left| i\left(f \sum_k \exp\left[i\mathbf{h} \cdot \mathbf{x}\,(k)\right]\right) \frac{\mathbf{h} \cdot \mathbf{u}\,(\mathbf{q})}{V_c}\right|^2 \tag{5}$$

where $\mathbf{u}(\mathbf{q}) = \int \mathrm{d}x\, u(x) \exp(iqx)$ is the Fourier transform of the elastic displacement field and $V_c$ denotes the volume of unit cell.

To compute $\mathbf{u}(\mathbf{q})$ and thence $I_H$ in various possible configurations of the interstitial in orthorhombic and tetragonal lattices, we use an extensively used model (Eshelby 1956) to simulate the stress field of the point defect. It is constructed by superposing

three orthogonal double forces without a twisting moment, *i.e.*, a symmetric double force tensor. A mathematical representation of such a force array will be

$$p_i(\mathbf{x}) = -P_{ij}\,\partial_j\,\delta(\mathbf{x}), \tag{6}$$

$x$ being measured with the position of the interstitial taken to be the origin. The symbols $i, j, k$ and $l$ represent the cartesian indices and the summation convention for the repeated indices is implied. $P_{ij} = K_i^n\,x_j^n$, is the force dipole tensor of the defect. It is the first moment of the Kanzaki force $\mathbf{K}^n$ on the atom $n$ (Dederichs *et al* 1978.) The dipole tensor depends mainly on the defect symmetry and can be calculated explicitly.

To calculate the elastic displacement field, we consider an infinite medium which possesses the symmetry of the Bravais lattice under consideration and is characterized by the relevant elastic constants. From the continuum theory of linear elasticity we have

$$\mathbf{C}_{ijkl}\,\partial_j\,\partial_l\,u_k(\mathbf{x}) = -p_i(\mathbf{x}) = P_{ij}\,\partial_j\,\delta(\mathbf{x}) \tag{7}$$

where $\mathbf{C}_{ijkl}$ is the elastic stiffness tensor. Fourier transformation of (7) gives the following expression for $\mathbf{u(q)}$

$$u_k(\mathbf{q}) = i\,D_{kl}^{-1}P_{ij}\,q_j \tag{8}$$

where $D_{ik} = \mathbf{C}_{ijkl}\,q_j\,q_l$. In general the computation of the actual displacement field of the defect by Fourier inverting $\mathbf{u(q)}$ involves assumptions regarding the anisotropy factor of the lattice. However, HDS circumvents these problems since it directly makes use of the transform $\mathbf{u(q)}$. Combining (5) and (8) we have

$$I_H = C\left(\frac{f}{V_c}\sum_k \exp\,[i\mathbf{h}\cdot\mathbf{x}(k)]\right)^2 |\,h_k\,D_{ki}^{-1}P_{ij}\,q_j\,|^2. \tag{9}$$

For a given defect configuration, HDS depends decisively on the inverse of the differential operator $D$. Elements of $D^{-1}$ for the least symmetric triclinic lattice with 21 independent elastic constants can be written as

$$D_{II'}^{-1} = \frac{\sum_{i,j,k,l}^{3} q_i\,q_j\,q_k\,q_l\,(\mathbf{C}_{iJJ'}\,\mathbf{C}_{kKIK'} - \mathbf{C}_{iJIK'}\,\mathbf{C}_{kKIJ'})}{\sum_{I''}^{3}\left(\sum_{j,l}^{3}\mathbf{C}_{JJ''}q_j\,q_l\right)\left(\sum_{i,j,k,l}^{3} q_i\,q_j\,q_k\,q_l\,(\mathbf{C}_{iJJ''}\,\mathbf{C}_{kKIK''} - \mathbf{C}_{iJIK''}\,\mathbf{C}_{kKIJ''})\right)} \tag{10}$$

The indices $I$ and $I'$ vary in cyclic manner, *i.e.* $(IJK)$ can have the following three sets of values (123), (231) and (312). Equation (10) represents the most general form of $D_{ij}^{-1}$ matrix. $D_{ij}^{-1}$ for different crystal structures can be obtained very easily from (10) by substituting the corresponding elastic constants.

## 3. Defect symmetry and topology of iso-intensity surfaces

Introduction of a point defect into a perfect crystal destroys the translational symmetry of the lattice. The defect symmetry is defined as the point group symmetry of this defective crystal. As the symmetry of the lattice cannot increase by the introduction of a defect, the defect symmetry is always lower than or equal to that of the perfect lattice. If the defective crystal has a symmetry lower than the perfect lattice, then there exist more than one distinguishable orientations of the defect configuration (Nowick and Berry 1972). In such a case, the contribution to HDS from all equivalent orientations of a given defect configuration must be appropriately averaged over. In order to specify the defect symmetry, one needs to know the symmetry elements which are common both to the defect when isolated from the crystal and to the site on the perfect lattice about which the defect is built. General nomenclature used to specify the defect symmetry (Nowick and Heller 1965), in terms of dipole force tensor of the defect, is tabulated in the appendix. Since HDS depends mainly on the long-range symmetry of the point defect, we shall focus our attention on the possible defect symmetries in orthorhombic and tetragonal lattices, instead of explicit defect configurations, for the purpose of calculating basic HDS profiles.

Due to the inversion symmetry of the elastic displacement field $[\mathbf{u}(\mathbf{r}) = -\mathbf{u}(-\mathbf{r})]$, there exists at least one nodal (zero-intensity) plane passing through each reciprocal lattice point across which Huang scattering amplitude changes sign. For various equivalent orientations of a given interstitial configuration, these nodal planes will be oriented differently and they may or may not coincide depending upon the symmetry of the defect. Curves of equal $x$-ray intensity can be computed numerically for model defects (Flocken and Hardy 1970) and iso-intensity curves compared with the measured $x$-ray scattering can yield the stable interstitial configuration. This procedure requires an extensive catalogue of iso-intensity curves for different materials and different defect symmetries. In order to avoid the effort of explicitly plotting the iso-intensity surfaces, we use, for brevity, a nomenclature introduced by Trinkaus (1972) to describe them: (i) double drop (*dd*)—if all the nodal planes coincide, giving rise to a double drop or multiple drop structure, (ii) apple-shaped (*as*)—if all the nodal planes intersect in a common line, giving rise to a line of zero intensity passing through the reciprocal lattice point, (iii) single bubble (*sb*)—if the nodal planes do not intersect in a common line, giving rise to a non-vanishing intensity at all points around the reciprocal lattice point.

## 4. Calculation of HDS

### 4.1 *Orthorhombic lattice*

4.1a *Defect sites and symmetries:* We choose [001] face of an orthorhombic lattice for illustration in figure 1. The point group symmetry of an orthorhombic lattice is $2/m\ 2/m\ 2/m$. A general site* $(x\ y\ z)$, unrelated to the crystallographic axes will possess triclinic symmetry. In a primitive orthorhombic lattice (figure 1a), a general point $y$ in the $x$-$y$ plane will have monoclinic symmetry. Sites $a$ at a cell corner, $f$ at

*The lattice sites are labelled according to a notation given to International Tables (1969).

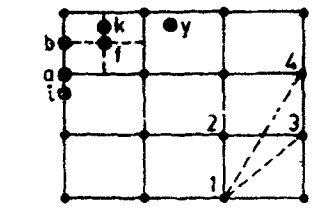


(a) P mmm

| Site | Symmetry |
|---|---|
| y | monoclinic |
| a, f, b, k, i | <100> orthorhombic |
| 1-2 pr. | <100> orthorhombic |
| 1-3 pr. | <110> orthorhombic |
| 1-4 pr. | monoclinic |

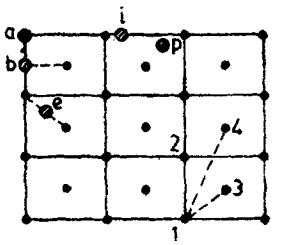


(b) C mmm

| Site | Symmetry |
|---|---|
| p | monoclinic |
| a, b, i | <100> orthorhombic |
| e | <110> orthorhombic |
| 1-2 pr. | <100> orthorhombic |
| 1-3 pr. | <110> orthorhombic |
| 1-4 pr. | monoclinic |

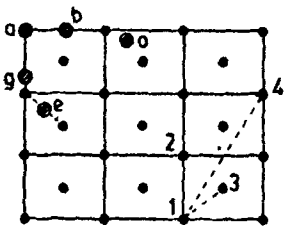


(c) F mmm

| Site | Symmetry |
|---|---|
| o | monoclinic |
| a, b, g | <100> orthorhombic |
| e | <110> orthorhombic |
| 1-2 pr. | <100> orthorhombic |
| 1-3 pr. | <110> orthorhombic |
| 1-4 pr. | monoclinic |

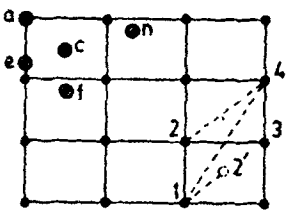


(d) I mmm

| Site | Symmetry |
|---|---|
| n | monoclinic |
| a, e, c, f | <100> orthorhombic |
| 1-2' pr. | <111> orthorhombic |
| 1-2 pr. | <100> orthorhombic |
| 2-4 pr. | <110> orthorhombic |
| 1-4 pr. | monoclinic |

**Figure 1.** Defect sites in an orthorhombic lattice: (a) primitive (b) c-centred (c) face centred (d) body centred.

a face centre and *b* at an edge centre have full orthorhombic symmetry. Points *k* and *i* have lower orthorhombic symmetry (*mm*2). For composite defects (*e.g.*, pairs, dumb-bells) the defect symmetry may be lower than or equal to that of the site symmetry. A pair placed at the points 1 and 2, or a dumb-bell aligned along the ⟨100⟩ axis will have orthorhombic symmetry. 1-3 pair will have a site symmetry of type *f* (equivalent to that of site *f*) and is ⟨110⟩ orthorhombic. A dumb-bell at positions 1 and 4 has a site symmetry of type *b*, but the overall defect symmetry is monoclinic due to [001] mirror plane.

In a *c*-centred orthorhombic lattice (figure 1b) an arbitrary point *p* in the *x*-*y* plane possesses monoclinic symmetry. Sites *a* at a cell corner, *i* at an arbitrary position along the *y* axis and *b* at an edge centre are ⟨100⟩ orthorhombic. Point *e* at one quarter along the face diagonal is ⟨110⟩ orthorhombic. Pair 1-2 has full orthorhombic symmetry and pair 1-3 has the site symmetry of type *e*. The site symmetry of 1-4 pair is [001] mirror plane, giving rise to a monoclinic symmetry.

In a face-centred orthorhombic lattice (figure 1c), an arbitrary point O in the *x*-*y* plane will have monoclinic symmetry. Sites *g* at an arbitrary position along a cell axis, *a* at a cell corner and *b* at an edge centre are ⟨100⟩ orthorhombic. Point *e* at one quarter along the face diagonal is ⟨110⟩ orthorhombic. Pair 1-2 is ⟨100⟩ orthorhombic and pair 1-3 has the site symmetry of type *e*. The 1-4 pair has monoclinic symmetry.

In a body-centred orthorhombic lattice (figure 1d), an arbitrary point *n* in the *x*-*y* plane has monoclinic symmetry. Sites *a* at a cell corner, *c* at a face centre have full orthorhombic symmetry, whereas an arbitrary point *e* on x-axis and point *f* have lower orthorhombic symmetry.

From the foregoing remarks we observe that three types of defect symmetries are permitted in an orthorhombic lattice: (i) triclinic, (ii) monoclinic and (iii) orthorhombic.

4.1b *Random distribution of equivalent orientations:* For an orthorhombic lattice, all equivalent orientations of an anisotropic defect configuration can be generated by a two fold rotation about the cartesian axes followed by a reflection in the mirror plane perpendicular to the rotation axis. The averaged HDS can then be written as

$$I_H = C\left(\frac{f\sum_K \exp\left[i\,\mathbf{h}\cdot\mathrm{x}\,(k)\right]}{V_c}\right)^2 \sum_{\nu=1}^{9} \pi_\nu\, r_\nu. \tag{11}$$

Independent constants $\pi_1 - \pi_9$, expressed in terms of the components of dipole tensor for any particular orientations are

$$\pi_1 = P_{11}^2;\ \pi_2 = P_{22}^2;\ \pi_3 = P_{33}^2;\ \pi_4 = P_{11}P_{22};\ \pi_5 = P_{11}P_{33};\ \pi_6 = P_{22}P_{33};$$

$$\pi_7 = P_{23}^2;\ \pi_8 = P_{13}^2;\ \pi_9 = P_{12}^2; \tag{12}$$

In table 1, we have given the values of the coefficients $r_\nu$ for some high symmetry directions and reflections. Wherever $r_\nu$ have simple forms, these have been explicitly given. More complicated expressions have been represented by the symbol *F* (for ' finite ') in order to identify all the $r_\nu$ which contribute to a particular reflection

**Table 1.** Values of the coefficients $r_\nu$ for some high reflections and directions in units of $(h/q)^2$. Lengthy algebraic expressions have been replaced by $F$ (for finite, non-zero values).

| Reflection | Direction of $q$ | $r_1$ | $r_2$ | $r_3$ | $r_4$ | $r_5$ | $r_6$ | $r_7$ | $r_8$ | $r_9$ |
|---|---|---|---|---|---|---|---|---|---|---|
| (h00) | [h00] | $C_{11}^{-2}$ | 0 | 0 | 0 | 0 | 0 | 0 | 0 | 0 |
| | [0h0] | 0 | 0 | 0 | 0 | 0 | 0 | 0 | 0 | $C_{66}^{-2}$ |
| | [00h] | 0 | 0 | 0 | 0 | 0 | 0 | 0 | $C_{55}^{-2}$ | 0 |
| (0h0) | [h00] | 0 | 0 | 0 | 0 | 0 | 0 | 0 | 0 | $C_{66}^{-2}$ |
| | [0h0] | 0 | $C_{22}^{-2}$ | 0 | 0 | 0 | 0 | 0 | 0 | 0 |
| | [00h] | 0 | 0 | 0 | 0 | 0 | 0 | $C_{44}^{-2}$ | 0 | 0 |
| (00h) | [h00] | 0 | 0 | 0 | 0 | 0 | 0 | 0 | $C_{55}^{-2}$ | 0 |
| | [0h0] | 0 | 0 | 0 | 0 | 0 | 0 | $C_{44}^{-2}$ | 0 | 0 |
| | [00h] | 0 | 0 | $C_{33}^{-2}$ | 0 | 0 | 0 | 0 | 0 | 0 |
| (hh0) | [hh0] | F | F | 0 | F | 0 | 0 | 0 | 0 | F |
| (h0h) | [h0h] | F | 0 | F | 0 | F | 0 | 0 | F | 0 |
| (0hh) | [0hh] | 0 | F | F | 0 | 0 | F | F | 0 | 0 |

**Table 2.** Topology of isointensity surfaces. $P_\perp$ [100] indicates a plane of zero intensity perpendicular to the [100] direction. $L_\parallel$ [001] indicates a line of zero intensity parallel to the [001] direction.

| Defect symmetry | Orthorhombic | | Monoclinic | | Triclinic | |
|---|---|---|---|---|---|---|
| Reflection | Zero intensity surface | Topology of iso-intensity surfaces | Zero intensity surface | Topology of iso-intensity surfaces | Zero intensity surface | Topology of iso-intensity surfaces |
| (h00) | $P_\perp$ [100] | *dd* | $L_\parallel$ [001] | *as* | none | *sb* |
| (0h0) | $P_\perp$ [010] | *dd* | $L_\parallel$ [001] | *as* | none | *sb* |
| (00h) | $P_\perp$ [001] | *dd* | $P_\perp$ [001] | *dd* | none | *sb* |

in a given direction. In an orthorhombic lattice, it is possible to determine uniquely the components of the force dipole tensor of the defect, even for a random distribution of equivalent defect orientations.

4.1c *Topology of iso-intensity surfaces:* For defects of orthorhombic symmetry, the symmetry operations leave the dipole tensor unchanged. So the averaged value of the dipole tensor for all the equivalent orientations will be same as that for any particular orientation. Owing to this, all iso-intensity surfaces will be of the *dd* type for orthorhombic defects. We have listed in table 2 some high symmetry directions and reflections where the HDS tends to zero. The presence or absence of zero intensity planes or lines can be used to distinguish between different defect symmetries.

## 4.2 *Tetragonal lattice*

4.2a *Defect sites and symmetries:* The [001] face of a tetragonal lattice is illustrated in figure 2. The point group symmetry of a tetragonal lattice is 4/mmm. A general site $(x, y, z)$, unrelated to crystallographic axes will possess triclinic symmetry. In a primitive tetragonal lattice (figure 2a), a defect at an arbitrary point $p$ in the $x$-$y$ plane will have monoclinic symmetry. A defect placed along the x or y axis, at a site $n$ and at an edge centre ($f$) will be ⟨100⟩ orthorhombic. But the defect sites along the face diagonal are ⟨110⟩ orthorhombic. Sites $c$ at a face centre and $a$ at a cell corner have full tetragonal symmetry. A defect pair at sites 1 and 3 will have tetragonal symmetry, whereas defect pairs 1-2 and 1-4 will be ⟨100⟩ orthorhombic.

In a body-centred tetragonal lattice (figure 2b), a general site $l$ in the $x$-$y$ plane will have monoclinic symmetry. Sites $c, j$ and $i$ are ⟨100⟩ orthorhombic, whereas the site $h$ along the face diagonal is ⟨110⟩ orthorhombic. Defect along the $z$-axis and at a cell corner will have tetragonal symmetry. A defect pair at sites 1-2 and 1-4 are ⟨100⟩ orthorhombic, whereas a defect pair at sites 1-3 will be ⟨110⟩ orthorhombic.

Four defect symmetries are permitted in a tetragonal lattice: (i) tetragonal, (ii) orthorhombic, (iii) monoclinic and (iv) triclinic.

4.2*b Random distribution of equivalent orientations:* For a tetragonal crystal, the

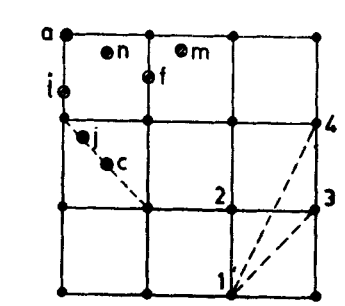


(a) P 4/mmm

| Site | Symmetry |
|---|---|
| m | monoclinic |
| l, n, f | <100> orthorhombic |
| j | <110> orthorhombic |
| c, a | tetragonal |
| 1-2 pr., 1-4 pr. | orthorhombic |
| 1-3 pr. | tetragonal |

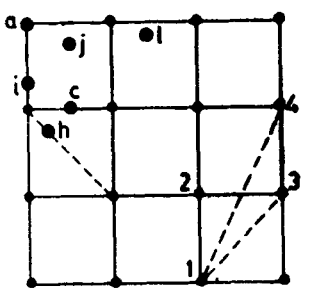


(b) I 4/mmm

| Site | Symmetry |
|---|---|
| l | monoclinic |
| j, l, i, c | <100> orthorhombic |
| h | <110> orthorhombic |
| a | tetragonal |
| 1-2 pr., 1-4 pr. | orthorhombic |
| 1-3 pr. | <110> orthorhombic |

**Figure 2.** Defect sites in a tetragonal lattice: (a) primitive (b) body-centred.

z-axis is unique. Thus the contribution to HDS from equivalent orientations need be averaged mostly in the basal plane. All equivalent orientations can be generated by a four-fold rotation about the z-axis, two-fold rotation about the x and y axis followed by an inversion in the mirror plane perpendicular to the rotation axis. The averaged HDS can then be written as

$$I_H = C\left(\frac{f}{V_c}\sum_k \exp\ [i\,\mathbf{h}\,.\,\mathbf{x}\,(k)]\right)^2 \sum_{\nu=1}^{6} \pi_\nu\, r_\nu \tag{13}$$

$\pi_\nu$ represent the six independent parameters in the tensor $P_{ij}\,P_{kl}$ and their specific forms are given below

$$\pi_1 = \tfrac{1}{2}\,(P_{11}^2 + P_{22}^2);\ \pi_2 = P_{33}^2;\ \pi_3 = P_{11}\,P_{22};\ \pi_4 = \tfrac{1}{2}\,P_{33}\,(P_{11} + P_{22});$$

$$\pi_5 = P_{12}^2;\ \pi_6 = \tfrac{1}{2}\,(P_{13}^2 + P_{23}^2) \tag{14}$$

The coefficients $r_\nu$ are listed in table 3 for some high symmetry reflections and directions.

4.2c *Topology of iso-intensity surfaces:* For a tetragonal lattice, the averaging is performed mainly in the basal plane leading to a mixing of $P_{11}$ and $P_{22}$ components. It is then not possible to distinguish between defects of tetragonal and ⟨100⟩ orthorhombic symmetry. Table 4 lists some high symmetry reflections and directions where the HDS tends to zero for some defect symmetries.

## 5. Discussion and concluding remarks

We have shown that in orthorhombic and tetragonal lattices, the point defects having different long-range symmetry can be clearly distinguished by measuring HDS

**Table 3.** Values of coefficients $r_\nu$ for some high symmetry directions and reflections in units of $(h/q)^2$. Lengthy algebraic expressions have been replaced by $F$ (finite).

| Reflection | Direction of $q$ | $r_1$ | $r_2$ | $r_3$ | $r_4$ | $r_5$ | $r_6$ |
|---|---|---|---|---|---|---|---|
| (h00) | [h00] | $C_{11}^{-2}$ | 0 | 0 | 0 | 0 | 0 |
| | [0h0] | 0 | 0 | 0 | 0 | $C_{66}^{-2}$ | 0 |
| | [00h] | 0 | 0 | 0 | 0 | 0 | $C_{44}^{-2}$ |
| (00h) | [h00] | 0 | 0 | 0 | 0 | 0 | $C_{44}^{-2}$ |
| | [00h] | 0 | $C_{33}^{-2}$ | 0 | 0 | 0 | 0 |
| (hh0) | [hh0] | F | 0 | F | 0 | F | 0 |
| (h0h) | [h0h] | F | F | 0 | F | 0 | F |

**Table 4.** Topology of iso-intensity surfaces in a tetragonal lattice.

| Defect symmetry | Tetragonal and orthorhombic | | Monoclinic | | Triclinic | |
|---|---|---|---|---|---|---|
| Reflection | Zero intensity surface | Topology of iso-intensity surface | Zero intensity surface | Topology of iso-intensity surface | Zero intensity surface | Topology of iso-intensity surface |
| ($h$00) | $P_\perp$ [100] | *dd* | $L_\parallel$ [001] | *as* | none | *sb* |
| (0$h$0) | $P_\perp$ [010] | *dd* | $L_\parallel$ [001] | *as* | none | *sb* |
| (00$h$) | $P_\perp$ [001] | *dd* | $P_\perp$ [001] | *dd* | none | *sb* |

about appropriately chosen reflections and directions. However for defects possessing identical long-range symmetry, additional information regarding the nature and the range of defect forces is necessary. For example, in an orthorhombic lattice, a point defect lying at a cell corner or at an edge centre or at a face centre has orthorhombic symmetry ($P_{11} \neq P_{22} \neq P_{33} \neq 0$; $P_{ij}=0$, $i \neq j$). An experimental measurement of HDS yields only the magnitude and the sign of dipole tensor elements. If the defect forces are short-ranged in nature (as can be guessed from the relaxation volume of the defect), than a nearest neighbour central force model gives a good approximation to the force array due to the defect. In such a case, elements of dipole force tensor can be calculated in a straightforward manner and a reasonable guess about the stable interstitial configuration can be made. For a strongly distorting defect, the dipole tensor depends sensitively on the nature and range of the potential used for the calculation (Kapoor 1980). In such a case assigning the experimental dipole tensor values to a particular defect configuration is quite ambiguous and the role played by HDS in identifying the stable interstitial configuration is rather restricted.

## Appendix

Effect of defect symmetry on the principal values and principal axes of the force dipole tensor $P_{ij}$.

| Defect Symmetry | Principal values | Principal axes | No. of independent $P_{ij}$ components |
|---|---|---|---|
| Cubic | $P_{11} = P_{22} = P_{33}$ | arbitrary | 1 |
| Tetragonal, Hexagonal and Trigonal | $P_{11} \neq P_{22} = P_{33}$ or $P_{11} = P_{22} \neq P_{33}$ | axis 1 along the major symmetry axis or axis 3 along the major symmetry axis | 2 |
| Orthorhombic | $P_{11} \neq P_{22} \neq P_{33}$ | along the three symmetry axes | 3 |

**Appendix** (contd.)

| | | | |
|---|---|---|---|
| Monoclinic | $P_{11} \neq P_{22} \neq P_{33}$ | axis 1 or 3 along the symmetry axis | 4 |
| Triclinic | $P_{11} \neq P_{22} \neq P_{33}$ | unrelated to crystal axes | 6 |

## References


Dederichs P H 1973 *J. Phys.* **F3** 471

Dederichs P H, Lehmann C, Schober H R, Scholz A and Zeller R 1978 *J. Nucl. Mater.* **69-70** 176

Ehrhart P and Schonfeld B 1979 *Phys. Rev.* **B19** 3896

Eshelby J D 1956 in *Solid state physics* (ed) F Seitz and D Turnbull (New York: Academic Press) Vol. 3

Flocken J W and Hardy J R 1970 *Phys. Rev.* **B1** 2472

Haubold H G 1975 in *Fundamental aspects of radiation damage in metals, Proc. Int. Conf. Gattinburg*, (eds) M T Robinson and F W Young (Springfield: U S Department of Commerce)

International *Tables for x-ray crystallography* Vol. I 1969 (eds) F M Norman Henry and K Lonsdale (Birmingham: Kyonoch Press)

Kapoor R 1980 *Pramana* **14** 209

Nowick A S and Heller W R 1965 *Adv. Phys.* **12** 251

Nowick A S and Berry B S 1972 *Anelastic relaxation in crystalline solids* (New York: Academic Press)

Trinkaus H 1972 *Phys. Status Solidi* **B51** 307